# APPLICATION OF SINUSOIDAL CURVES TO SHAPE DESIGN OF CHORD SOUND PLATE AND EXPERIMENTAL VERIFICATION

Bor-Tsuen Wang, Yong-Shiang Hsu, Shao-Wei Cheng, Chian-Hong Chen, Chia-Hsien Huang, and Ying-Hui Wu

*Department of Mechanical Engineering, National Pingtung University of Science and Technology, Pingtung, 91201, Taiwan*
*e-mail:wangbt@mail.npust.edu.tw*

This work reviews the design concept of chord sound plate (CSP) that is a uniform thickness plate with special curved shape designed by Bezier curve (B-curve) method. The CSP can generate the percussion sound with three tone frequencies that consist of the musical note frequencies of triad chord. This work proposes the new design concept by adopting dual sine-wave curve (S-curve) to obtain the optimum shape of CSP that can still generate triad chord sound properly. The shape design method from B-curve to S-curve for the CSP is first introduced. The optimization problem in designing the S-curve CSP is then formulated and shown for the optimal solution procedure involving structural modal analysis. The S-curve design CSP is manufactured and performed experimental modal analysis (EMA) to obtain the plate's natural frequencies and mode shapes so as to validate the design of CSP. Results show the percussion sound response of CSP with one strike on the plate can generate the triad sound by examining the sound spectrum. The S-curve design method is shown feasible to obtain the proper design of CSP and advantage over the B-curve method. The design methodology of CSP can be extended to other triad chords, and the chord sound plates are potential for the commercial percussion instrument.

Keywords: chord sound plate (CSP), shape optimization, modal analysis, percussion instrument, sound spectrum.

## 1. Introduction

Percussion instrument is one type of musical instrument that is mainly due to structural vibration modes; therefore, theoretical modal analysis (TMA) and experimental modal analysis (EMA) are frequently adopted to study and design the percussion instruments. Bretos *et al*. [1] use finite element analysis (FEA) to determine vibration modes of wooden bars used in musical instrument and measured the structural natural frequencies. Petrolito and Legge [2] developed optimization method to tune the percussive beam by varying special undercut shape. The numerical model on the beam structure is analysed to obtain the modes of vibration. McLachlan [3] also adopted FEA for the design of musical bells and performed EMA on the bell to validate the structural vibration modes. Ansari [4] also used the FEA and EMA to calibrate bell model to predict the fundamental frequency and those overtone frequencies.

Since the structural vibration modes dominate the effect of percussion sound, the geometry study and design for percussion instrument are of interest. Jing [5] presented the study on ancient Chinese bell for both sound and vibration characteristics. The geometry effect was shown to identify the tone frequency of bell as well as the small decay effect due to flat shape cross section. Wang and Chang [6] showed a steel chime study similar to the ancient Chinese chime with L shape plate.

They indicated that sound effect of steel chime is harmonics, i.e. the overtone frequencies and the fundamental frequency with integer ratios. Wang and Tsai [7] discussed the percussion sound of flat gong and found that different percussion locations from the centre of gong to the edge will result in different sound effects due to the structural vibration mode shapes. The percussion location and structural mode shapes are correlated and the key issues for percussion instrument design. Boullosa [8] adopted EMA technique and measured the sound spectrum for different sound board material of classical guitars. The sound board materials will also affect the play sound response.

To produce the chord sound for percussion instruments such as xylophone or metalophone, the player has to use three sticks to strike simultaneously on the related musical notes in order to play the triad sound. Wang *et al*. [9] have the design of chord sound plate (CSP) that can produce the triad sound with one strike on the CSP. The CSP design is carried out the shape optimization by Bezier curve (B-curve) that is not easy for redesign of the shape for different musical notes. How to perform the optimal design of geometry shape of CSP effectively and efficiently is a challenge. This work proposes the new design strategy by adopting the dual sine-wave curve (S-curve) instead of Bezier curve (B-curve).

Wang and Hsieh [10] presented two types of metal bars that can generate the chord sound, and the patent was filed [9]. The B-curve method is adopted for geometry optimization. Wang and Jian [11] showed the design verification of one type of Metallophone with chord sound by using finite element analysis (FEA) and experimental modal analysis (EMA) techniques to obtain theoretical and experimental modal parameters, respectively. Results showed that the numerical FE model can be equivalent to the practical chord sound plate (CSP). Modal analysis on the plate vibration modes is working well in predicting the percussion sound for the design of CSP. Although the B-curve method is working well on the design of CSP, the design variables are not patterned and so forth the optimization process is difficult to trace.

Wang *et al*. [12] proposed the new method by using multiple sine waves to formulate the geometry shapes of sound plate, in particular for harmonic sound plate (HSP). In this work, we adopt dual sine-wave to mimic the original design of CSP [9]. The optimum parameters for designing CSP can be physically interpreted from the dual-sine wave variables. The purposes of the study are as follows:

(1) **Design analysis for CSP**: the geometry shape design of CSP is carried out by dual-sine wave curve (S-curve) method instead of Bezier curve (B-curve) method.

(2) **Model verification of CSP**: the new designed shape of CSP is fabricated and performed EMA to obtain modal parameters to validate the design model.

(3) **Percussion sound of CSP**: other than to correlate the sound effect related to vibration modes of one CSP, we show four types of triad CSPs, i.e. C major, C minor, C diminished and C augmented, to examine the sound spectrum.

## 2. Optimum design of chord sound plate

This section will briefly review the B-curve method for CSP, and then the S-curve method will be shown. Design parameters between B-curve and S-curve methods are properly transferred base on the original shape of CSP [9]. The geometry optimization problem can then be formulated base on S-curve method.

### 2.1 B-curve method

Fig. 1(a) shows the design of CSP that is symmetry in y-direction, and Fig. 1(b) shows the conceptual plot for Bezier curve (B-curve) method for the upper half geometry of CSP [9]. Fig. 1(b) shows there are $n+1$ control points ( $p_i$ ) that are known and $m$ Bezier points $\overline{p}_j$ . The coordinates are designated as follows:

$$p_i = (x_i, y_i), i = 0,1,...,n .$$ (1)

$$\overline{p}_j = \left( \overline{x}_j, \overline{y}_j \right), j = 0,1,...,m. \tag{2}$$

where

$$\overline{x}_j = \sum_{i=0}^{n} \binom{n}{i} (1-u_j)^{n-i} u_j^i x_i \quad . \tag{3}$$

$$\overline{y}_j = \sum_{i=0}^{n} \binom{n}{i} (1-u_j)^{n-i} u_j^i y_i \quad . \tag{4}$$

$$\binom{n}{i} = \frac{n!}{i!(n-i)!}. \tag{5}$$

$$u_j = \frac{j}{m}. \tag{6}$$

In designing the CSP, the coordinates of control points shown in Eq. (1) are design variables having the number of $2(n+1)$. From the control point locations, all Bezier points shown in Eq. (2) can be determined and formed the smooth curve that is depicted by asterisks in Fig. 1(b) and the upper half geometry of CSP as shown in Fig. 1(a)
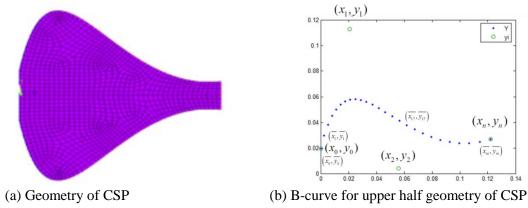


(a) Geometry of CSP  (b) B-curve for upper half geometry of CSP

Figure 1: Bezier curve (B-curve) design method for CSP.

## 2.2 Transformation from B-curve to S-curve

The S-curve method proposed by Wang *et al*. [12] uses the concept similar to Fourier series. The dual-cosine wave equation is as follows:

$$y(x) = y_0 + y_1(x) + y_2(x)$$
$$= y_0 + A_1 \cos\left( 2\pi \frac{x}{\lambda_1} + \phi_1 \right) + A_2 \cos\left( 2\pi \frac{x}{\lambda_2} + \phi_2 \right). \tag{7}$$

Fig. 2(a) depicts $y(x)$ and those individual curves including $y_0$ the constant value, and $y_1(x)$ and $y_2(x)$ the two cosine waves, respectively. $A_i$, $\lambda_i$ and $\phi_i$ are the amplitude, wave length and phase angle of the *i*-th cosine wave. With the proper selection of cosine wave variables and the constant $y_0$, the corresponding curve for the CSP geometry can be obtained.

For the CSP design by B-curves, those control points are known and can be used to construct the Bezier point coordinates that are also known in priori. The objective here is to obtain the S-curve that can be constructed by $y_0$, $A_i$, $\lambda_i$ and $\phi_i$ such that both S-curve and B-curve will be as close as possible. The least mean square error method is adopted to formulate the objective function of optimization problem as follows:

$$OBJ = \sqrt{\frac{1}{N_p}\sum_{i=1}^{N_p}\left(\frac{y(x_i)-y_b(x_i)}{y_b(x_i)}\right)^2}.$$ (8)

$y(x)$ and $y_b(x)$ designate for the coordinates of S-curve and B-curve, respectively. $N_p$ is the number of data points. Fig. 2(b) shows the example for transformation of B-curve to S-curve.
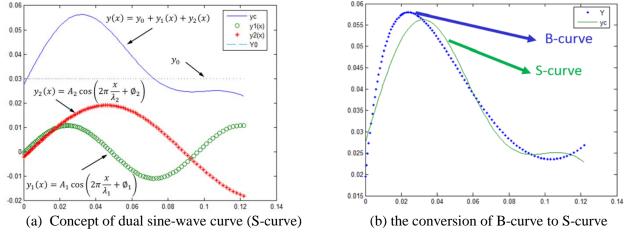


(a) Concept of dual sine-wave curve (S-curve)  (b) the conversion of B-curve to S-curve

Figure 2: Comparison of CSP shape from the conversion of B-curve to S-curve.

## 2.3  Optimization formulation of CSP design by S-curve

From the previous section, the new design concept for CSP by S-curve has been proposed; this section will formulate the optimization problem for the CSP geometry design. To define the optimization problem, one will detail the followings:

(1)  Design variables: for adopting S-curve, the design variables include those S-curve parameters, the design variable set can be written as follows:

$$X = \{y_0, A_1, \lambda_1, \phi_1, A_2, \lambda_2, \phi_2\}.$$ (9)

(2)  Objective function: Here, we want to design the CSP, i.e. the chord sound such as C major triad containing C, E and G notes. Let $f_{obj1}$, $f_{obj2}$ and $f_{obj3}$ be the target frequencies for C major triad. The initial guess of design variables can result in the first three modal frequencies of the pre-shaped CSP, e.g. $f_1$, $f_2$ and $f_3$. The design goal is to find the design variables such that the plate natural frequencies will coincide with the standard frequencies of musical notes; therefore, the objective function can be formulated base on least root mean square error between natural frequencies and musical notes' frequencies and defined as follows:

$$F(X) = \sqrt{\frac{1}{3}\sum_{r=1}^{3}\varepsilon_r^2} = \sqrt{\frac{1}{3}\left[\left(\frac{f_1-f_{obj1}}{f_{obj1}}\right)^2+\left(\frac{f_2-f_{obj2}}{f_{obj2}}\right)^2+\left(\frac{f_3-f_{obj3}}{f_{obj2}}\right)^2\right]}.$$ (10)

Where the r-th mode frequency error can be written as follows:

$$\varepsilon_r = \frac{f_r-f_{obj,r}}{f_{obj,r}}\times 100\%.$$ (11)

(3)  Constraints: The design of CSP should have the exact frequency response or within the acceptable range of error. Each mode of frequency error is the constraint and written as follows:
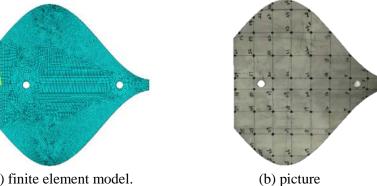
$$-0.34\% < \varepsilon_r < 0.34\% \, . \tag{12}$$

With the above formulation for optimization problem of CSP geometry design, the finite element model can be constructed by using S-curve method with parametric formulation and performed modal analysis to obtain natural frequencies, $f_r$. This is the forward analysis. Then, by using the ANSYS software optimization toolbox, the reverse design analysis to determine the optimum set of design variables can be preceded with the above formulation.

## 3.   Design verification of CSP via S-curve method

Figs. 3(a) and 3(b) shows finite element model and real structure of the new design of CSP for C minor via S-curve method. Once the optimum design is complete, the CSP is manufactured by laser cut according to the precise geometry shape. Fig. 4(a) shows the experimental setup for experimental modal analysis (EMA) on the CSP, while Fig. 4(b) reveals the 60 grid points on the CSP. The Sound and Vibration Measurement (SVM) software in conjunction with data acquisition device NI-9234 is applied to capture the hammer force and acceleration response that are processed to obtain the frequency response function (FRF). The accelerometer is fixed at Point 1, while the impact hammer is roving over the 60 grid points; therefore, 60 sets of FRFs can be determined and input to ME'scopeVES for curve-fitting to obtain structural modal parameters, including natural frequencies, mode shapes and modal damping ratios.

Fig. 5 shows the comparison of FRFs for the C minor CSP. There are three curves in Fig. 5. That the "synthesized" FRF agrees with the "experimental" FRF indicates the reasonable post-processing of curve fitting; therefore, the obtained experimental modal parameters can be reasonable and reliable. The "FEA" FRF curve can be seen also comparable to the "experimental", i.e. the simulation on the CSP is good and equivalent to the real structure.
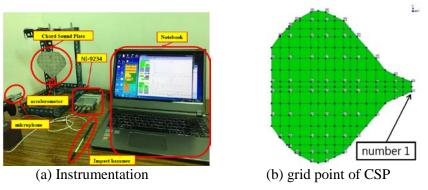


(a) finite element model.             (b) picture

Figure 3: The CSP for C minor.



(a) Instrumentation             (b) grid point of CSP

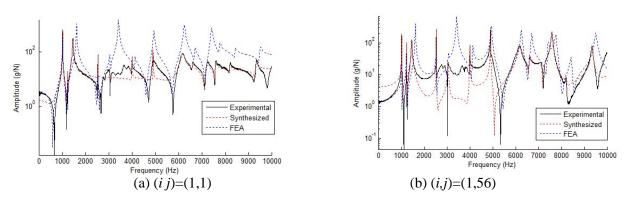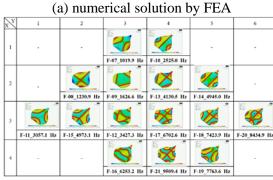Figure 4: Experimental setup for EMA on the CSP.

(a) (*i j*)=(1,1)  (b) (*i,j*)=(1,56)

Figure 5: $H_{ij}(f)$, FRF of the CSP.

Table 1: Comparison of modal parameters between FEA and EMA.

| EMA | | FEA | | Frequency error (%) | MAC | Damping ratio (%) | Physical meaning of mode shapes (X,Y) |
|---|---|---|---|---|---|---|---|
| Mode No. | Natural frequency (Hz) | Mode No. | Natural frequency (Hz) | | | | |
| E-01 | 1022.1 | F-07 | 1019.9 | 0.216 | 0.932 | 0.136 | (1,3) |
| E-02 | 1241.1 | F-08 | 1230.9 | 0.829 | 0.894 | 0.045 | (2,2) |
| E-03 | 1463.9 | F-09 | 1626.6 | -10.002 | 0.927 | 0.991 | (2,3) |
| E-04 | 2536.0 | F-10 | 2525.0 | 0.436 | 0.685 | 0.019 | (1,4) |
| E-05 | 3048.1 | F-11 | 3057.1 | -0.294 | 0.852 | 0.403 | (3,1) |
| -- | -- | F-12 | 3427.3 | -- | -- | -- | (3,3) |
| E-06 | 4002.1 | F-13 | 4130.5 | -3.109 | 0.898 | 0.092 | (2,4) |
| -- | -- | F-14 | 4945.0 | -- | -- | -- | (2,5) |
| E-07 | 4905.4 | F-15 | 4973.1 | -1.361 | 0.628 | 0.049 | (3,2) |
| E-08 | 6183.2 | F-16 | 6253.2 | -1.119 | 0.784 | 1.22 | (4,3) |
| E-09 | 6605.3 | F-17 | 6702.6 | -1.452 | 0.790 | 0.490 | (3,4) |
| E-10 | 7185.4 | F-18 | 7423.9 | -3.213 | 0.727 | 0.940 | (3,5) |
| E-11 | 7591.2 | F-19 | 7763.6 | -2.221 | 0.799 | 0.350 | (4,5) |
| E-12 | 8216.1 | F-20 | 8434.9 | -2.594 | 0.797 | 0.259 | (3,6) |
| E-13 | 9343.8 | F-21 | 9509.4 | -1.741 | 0.796 | 0.327 | (4,4) |

Table 2: Comparison of modal parameters between FEA and EMA.

(a) numerical solution by FEA  (b) experimental solution by EMA
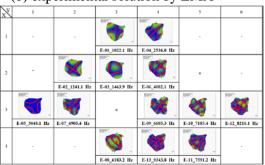


Table 1 summarizes the comparison of natural frequencies between FEA and EMA and modal damping ratios. The frequency errors are generally smaller than 3%, but only that of the E-03 and F-09 modes is about -10% due to the accelerometer mass effect. In Table 1, modal assurance criterion (MAC) values for the comparison of mode shapes between FEA and EMA are also shown. The MAC values for those low frequency modes are nearly above 0.9 indicating the match of physical meaning of mode shapes. Table 2(a) and 2(b) show the modes shapes obtained from FEA and EMA, respectively. Although the CSP is bottle-neck type of shape, the mode shapes of CSP can still be categorized as (X,Y) modes such as a rectangle plate. The physical meaning of mode shapes are noted in Table 1, and Table 2(a) and 2(b) reveal those mode shapes in (X,Y) sequence. One can observe the very good agreement between FEA and EMA. In summary, based on the good agreement between theoretical and experimental modal parameters, the numerical model of CSP can be

well calibrated and applied to other types of CSP design. It is also noted that natural frequencies of the first three modes are just corresponding to the standard frequencies of C minor chord sound.

Table 3: Definition of triad chords, e.g. C chords.

| Chord name | Component intervals | | Example | Chord symbol |
|---|---|---|---|---|
| Major triad | major third | perfect fifth | C-E-G | C, CM, Cma, Cmaj, C $\Delta$ |
| Minor triad | minor third | perfect fifth | C-E$^b$-G | Cm, Cmi, Cmin |
| Augmented triad | major third | augmented fifth | C-E-G$^{\#}$ | C+, C+, Caug |
| Diminished triad | minor third | diminished fifth | C- E$^b$- G$^b$ | Cm($^b$5), C°, Cdim |



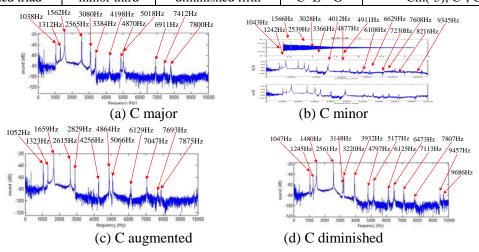(a) C major



(b) C minor



(c) C augmented



(d) C diminished

Figure 6: Sound spectrum for four CSPs.

Table 4: Comparison of peak frequencies of sound spectrum with target frequencies of C chords.

| Mode No. | C Major triad | | | | | C Minor triad | | | | |
|---|---|---|---|---|---|---|---|---|---|---|
| | Peak Frequency (Hz) | Frequency ratio | Target Frequency (Hz) | Frequency ratio | Frequency Difference (%) | Peak Frequency (Hz) | Frequency ratio | Target Frequency (Hz) | Frequency ratio | Frequency Difference (%) |
| S-01 | 1038 | 1 | 1046.50 | 1 | -0.812 | 1043 | 1 | 1046.50 | 1 | -0.334 |
| S-02 | 1312 | 1.264 | 1318.51 | 1.260 | -0.493 | 1242 | 1.191 | 1244.51 | 1.189 | -0.201 |
| S-03 | 1562 | 1.505 | 1567.98 | 1.498 | -0.381 | 1566 | 1.501 | 1567.98 | 1.498 | -0.126 |
| Mode No. | C Augmented triad | | | | | C Diminished triad | | | | |
| | Peak Frequency (Hz) | Frequency ratio | Target Frequency (Hz) | Frequency ratio | Frequency Difference (%) | Peak Frequency (Hz) | Frequency ratio | Target Frequency (Hz) | Frequency ratio | Frequency Difference (%) |
| S-01 | 1052 | 1 | 1046.50 | 1 | 0.525 | 1047 | 1 | 1046.50 | 1 | 0.047 |
| S-02 | 1323 | 1.258 | 1318.51 | 1.260 | 0.340 | 1245 | 1.189 | 1244.51 | 1.189 | 0.039 |
| S-03 | 1659 | 1.577 | 1661.22 | 1.587 | -0.133 | 1480 | 1.414 | 1479.98 | 1.414 | 0.001 |

## 4.  Sound measurement for different CSPs

This work is to show that the CSP can be designed and manufactured by S-curve. The most important part is to examine if the percussion sound of the CSP can produce the expected triad chord sound response. There are four types of triad chords, i.e. major, minor, augmented and diminished, as shown in Table 3 for detail definition and composition of musical notes about C chords. This work shows the CSPs for the four triads for C chords.

Figs. 6(a)-(d) show the sound spectrum of CSPs for C major, C minor, C augmented and C diminished triad chords. The first three frequencies measured for the four pieces of CSPs are summarized in Table 4. One can observe that the frequency errors between the peak frequency and target frequency are very small and generally less than 1%. The C minor and C diminished chords can fulfil the target frequencies for all three target modes within 0.34%, i.e. the design and manufacture of CSPs are successful. The fundamental frequencies of C major and C augmented are slightly higher than the requirement of 0.34% frequency error; however, the frequency ratios for the three

musical notes are quite close to the desired. In summary, this work applies the S-curve method to obtain the CSPs design that is basically good for the design goal. The minor difference in frequency error may be due to the manufacturing error and can be adjusted as desired accordingly.

## 5. Conclusions

This work reviews the design concept of chord sound plate (CSP). Due to the design difficulty in using the Bezier curve (B-curve), this work employs the dual sinusoidal wave curve (S-curve) for the design of CSP. Results show the S-curve design method can successfully produce the optimum shape of CSP that can generate the chord sound. The designed triad CSP contains three musical notes in harmony. According to the optimum design, the CSP is produced and performed EMA to verify the physical design of CSP that has the expected modal properties and can generate three tone frequencies as the triad sound. The CSPs are made for different triads, including C major, C minor, C augmented and C diminished. The percussion sound is measured to validate the design of CSPs and revealed reasonable agreement with the prediction and, most importantly, with the musical note's standard frequencies. This work shows the S-curve method is promising in geometry design, in particular the CSP design is presented in this work.

## ACKNOWLEGEMENT

## REFERENCES

1  Bretos, J., Santamaria, C., and Moral, J. A., Finite Element Analysis and Experimental Measurements of Natural Eigenmodes and Random Responses of Wooden Bars Used in Musical Instruments, *Applied Acoustics*, 56, 141-156, (1999).

2  Petrolito, J., and Legge, K.A., Optimal Undercuts for the Tuning of Percussive Beams, *Journal of Acoustical Society of America*, 102(4), 2432-2437, (1997).

3  McLachlan N., The application of new analyses and design methods to musical bells, *75th Acoustical Society of America Conference*, New York, 1-8, (2004).

4  Ansari J., Finite Element Vibration Analysis and Modal Testing of Bells, *Proceedings of the 2006 IJME-INTERTECH Conference*, Union, NJ, USA, (2006).

5  Jing, M., A theoretical study of the vibration and acoustics of ancient Chinese bells, *Journal of the Acoustical Society of America*, 114(3), 1622-1628, (2003).

6  Wang, B. T., Chang, M. H., Mode Verification and Percussion Sound Characteristics of Steel Chime, *The 4th Cross–Strait Symposium on Dynamics, Vibration and Control*, Kaohsiung,  D-02, (2015). (in Chinese)

7  Wang, B. T., and Tsai, Y. L., Discussions on sound characteristics and vibration analysis of flat gong, *The 36th National Conference on Theoretical and Applied Mechanics,* Taoyuan, F-002, (2012). (in Chinese)

8  Boullosa, R. R., Vibration Measurement in the Classical Guitar, *Applied Acoustics*, 62, 311-322, (2002).

9  Wang, B. T., Chao, T. C., and Hsieh, M. H., 2016, *Manufacturing Method for a Metallophone with a Chord Plate and a Chord Plate of Metallophones*, Taiwan Patent No. I 409801, Date of Patent: 02/01/2013, Effective Date: 08/26/2028.

10  Wang, B. T., and Hsieh, M. H., Sound Characteristics and Design Analysis of the Metallophone Bar with Chord, *Conference on 2009 Annual Meeting and 22th Symposium of Acoustical Society of the Republic of China* ,Taipei, A006, (2009). (in Chinese)

11  Wang, B. T., and Jian, X. M., Model Verification and Percussion Sound Characteristics of Metallophone with Chord Sound, *The 17th International Congress on Sound and Vibration*, Cairo, Egypt, 376, (2010).

12  Wang, B. T., Dung, S. P., Wu, M. F., Tsai, Y. L., Chang, C. H., 2016, *Method for Design a Board with Harmonics Sound and Percussion Instruments with Boards* , Taiwan Patent No. I 530939, Date of Patent: 04/21/2016, Effective Date: 08/20/2034.